Oxidation Behavior of a SPS Sintered ZrB_2-SiC-$MoSi_2$ Ceramic at 1500 ^{0}C

Qi LI[1,a], Lamei CAO[1,b] and Xiaosu YI[1,c]
[1]Science and Technology on Advanced High Temperature Structural Materials Laboratory, Beijing Institute of Aeronautical Materials, Beijing 100095, China
[a]liqi1988china@126.com[1], [b]lamei.cao@biam.ac.cn, [c]yixs@avic.com

Abstract. ZrB_2-SiC-$MoSi_2$ ceramic (ZSM) was successfully prepared by SPS sintering process. The micro-structure and mechanical property were characterized, the oxidation behavior of ZSM was mainly studied at 1500 ^{0}C in air. Compared to ZrB_2-SiC ceramic (ZS), the mechanical property of ZSM was improved significantly. MoB phase increasing the mechanical and chemical bonding force between different phases was formed in ZSM during SPS sintering. After 10 h oxidation at 1500 ^{0}C in air, oxide layer thickness of ZSM was thinner than ZS, oxidation resistance of ZSM was better than ZS.

1. Introduction

In recent years, ZrB_2-SiC ceramic have become one of the most attractive candidate materials for the thermal protection system of the next generation hypersonic vehicles due to its high melting points, high strength, high thermal conductivity and relatively low density[1,2,3,4]. During supersonic flight and re-entry process, ZrB_2-SiC ceramic will serve in extremely harsh oxidative environment at high temperature. Therefore, the oxidation behavior of ZrB_2-SiC ceramic at high temperature was very important for its application. Researchers around the world have conducted a lot of work to study the oxidation behavior of ZrB_2-SiC ceramic and studies show that adding a suitable amount of refractory metal compounds as the third phase in ZrB_2-SiC ceramic might increase the oxidation resistance[5,6,7,8]. The oxidation behaviors of some ternary composite ceramics system, such as ZrB_2-SiC-TaC[9], ZrB_2-SiC-$ZrSi_2$[10], ZrB_2-SiC-$TaSi_2$[11], ZrB_2-SiC-LaB_6[12], ZrB_2-SiC-ZrO_2[13] and so on, have been researched intensively. $MoSi_2$ was found to be an effective additive to improve the sinterability and oxidation resistance of ZrB_2 ceramic[14,15,16], the oxidation behavior of ZrB_2-$MoSi_2$ ceramic has been studied[17,18]. However, the oxidation behavior of ZrB_2-SiC-$MoSi_2$ ceramic at high temperature was rarely reported.

In this article, ZrB_2-SiC-$MoSi_2$ ceramic (ZSM) was successfully prepared by spark plasma sintering (SPS), the mechanical property and oxidation behavior were characterized and compared with ZrB_2-SiC ceramic (ZS) prepared at the same condition. At 1500 ^{0}C in air, the mass gain at different oxidation time and the cross section analysis after oxidizing for 10 h were mainly studied to research the oxidation mechanism and the effect of $MoSi_2$ during

* Corresponding author: liqi1988china@126.com

the oxidation. The results could give technical support for the reliably application of ZSM in hash environment.

2. Experiment

Commercial powders were used to prepare the ceramics. ZrB_2, particle size: 10-15μm, purity: 99.5%; α-SiC, particle size: 2 μm, purity: 99.9 %; $MoSi_2$, particle size: 2 μm, purity: 99.9 %.

SPS Sintering to Prepare ZSM and ZS. The powder mixtures mixed with a certain volume proportion (ZrB_2: SiC: MoSi2=7:3:2 for ZSM; ZrB_2: SiC=7:3 for ZS) were filled into the ZrO_2 jar and ball milled for 6 h using ZrO_2 media. Subsequently, the slurries were dried in a rotary evaporator. The dried powder mixtures were filled into a graphite die, which was then put into the SPS furnace under argon atmosphere to sinter for 5 min at 1900 ^{0}C, with a heating rate of 100 ^{0}C/min and an applied pressure of 30 MPa.

Measurement. Apparent density was calculated by the mass and volume of the dried sample.

Vickers microhardness (HV 0.5) was measured with a load of 4.9 N on a hardness tester. Three-point bending strengths were measured on a INSTRON 3365 bending tester with 30 mm span and 0.5 mm/min rate of head movement. Three-point bending strength at 1600 ^{0}C was tested on a YKM-2200 bending tester with 30 mm span and 0.5 mm/min rate of head movement, the heating rate was 40 ^{0}C/min, holding time was 10 min. The microstructure and phase composition of ceramics are studied using the XRD method and a Nova Nano scanning electron microscopy (SEM). The chemical composition of the phases formed was inferred from energy dispersive X-ray spectroscopy (EDX). The oxidation experiments were carried out on a tube furnace in air.

3. Results and Discussions

Characterization. ZrB_2-30 vol.% SiC-20 vol.% $MoSi_2$ ceramic (ZSM) and ZrB_2-30 vol.% SiC ceramic (ZS) were successfully prepared via SPS sintering at 1900 ^{0}C. The density was calculated, the hardness, three-point bending strength at room temperature and high temperature were measured and shown in Table 1. The density of ZSM and ZS were both higher than 5 g/cm^3, close to their theoretical densities. The hardness of ZSM and ZS were 17.2 and 19.6 GPa, separately. The three-point bending strength of ZSM (361.6 MPa) was much higher than ZS (171.6 MPa) at room temperature. At 1600 ^{0}C, the strength of ZSM decreased significantly to 130.8 MPa, while the strength of ZS remained about the same (170.1 MPa). By adding a 20 vol.% $MoSi_2$ into ZS, the strength at room temperature increased significantly while it decreased apparently at 1600 ^{0}C.

TABLE 1 PARAMETERS OF AS-SINTERED ZSM AND ZS CERAMIC

Material	ZS	ZSM
Theoretical density [g/cm^3]	5.4	5.5
Apparent density [^{0}C]	5.3	5.2
Hardness (HV0.5) [GPa]	19.6	17.2
Three-point bending strength (25 ^{0}C) [MPa]	171.6	361.6
Three-point bending strength (1600 ^{0}C) [MPa]	170.1	130.8

Microstructures. To investigate the effect of $MoSi_2$, XRD patterns, SEM images and EDX analysis of ZSM and ZS were measured to analyze the microstructure and phase composition. XRD pattern of ZS (Fig. 1(a)) revealed that it was formed by two phases, ZrB_2 and SiC. SEM image (Fig. 1(b)) show the microstructure of ZS that the distribution of ZrB_2 and SiC were uneven. EDX results indicated that the white phase (1 area) in Fig. 1(b) was composed of ZrB_2, the gray phase (2 area) was composed of SiC, the black area (3 area) was pore. In ZS, the grain size distribution of ZrB_2 could range from 1 μm to 70 μm, while SiC grain aggregated in some regions, which was because SiC were uniformly dispersed in ZrB_2. The EDX results also revealed that ZrB_2 phase contained a small amount of O element which might be induced by ZrO_2 on the particle surface of ZrB_2 and ZrO_2 media used in ball mill.

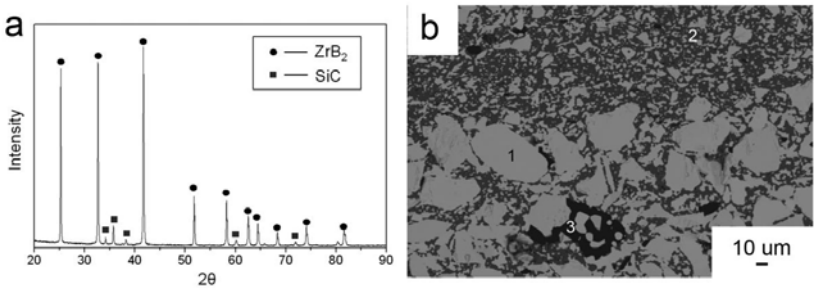

Fig. 1. XRD spectrum (a) and SEM image (b) of as-sintered ZS ceramic.

The XRD pattern and SEM images of ZSM are shown in Fig. 2. XRD pattern of ZSM (Fig. 2(a)) revealed that it was formed by three phases, ZrB_2, SiC and MoB. SEM image (Fig. 2(b)) show the microstructure of ZS that it was formed by gray phase (1 area), black phase (2 area) and white phase (3 area). The three phases distributed evenly, no aggregation was observed, and there were very little pores. The EDX analysis showed that the gray phase was ZrB_2, black phase was SiC, and white phase was MoB. MoB was produced by the reaction of ZrB_2, $MoSi_2$ and ZrO_2 during SPS sintering [14,17]. The mechanical and chemical bonding forces between different phases were both increased due to the existence of MoB. The enhanced bonding force between different phases in ZSM made the increasing mechanical properties of ZSM.

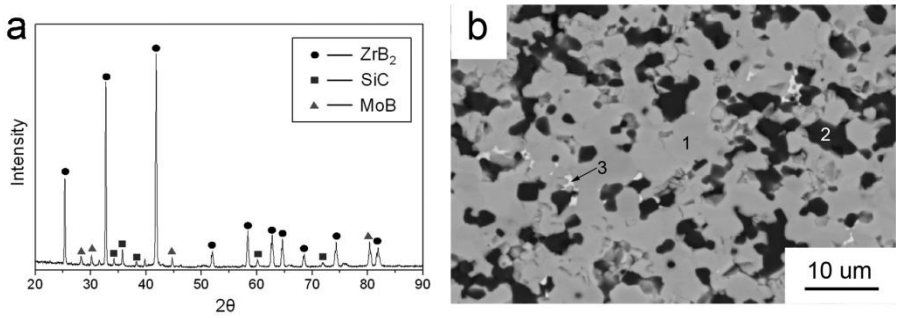

Fig. 2. XRD spectrum (a) and SEM image (b) of as-sintered ZSM ceramic.

The fracture morphology of ZSM and ZS were observed by SEM (Fig.3) to investigate the effect of $MoSi_2$ on the fracture mechanism. The fracture morphologies of ZSM and ZS performed quite different. The fracture of ZSM was intercrystalline and transcystalline mixed mode, but the fracture of ZS was only intercrystalline mode. The result showed that the toughness of ZSM was better than ZS.

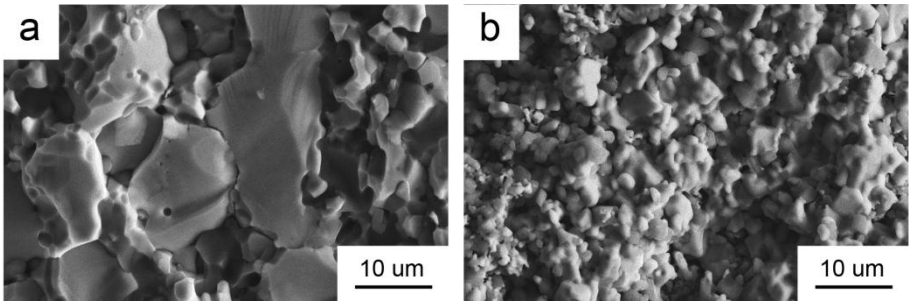

Fig. 3. Fracture morphologies of as-sintered ZS (a) and ZSM (b) ceramic.

Oxidation Behavior. At 1500 ^{0}C in air, ZSM and ZS were oxidized and weighted at different oxidation time. The changes of the mass gain were lined in Fig. 4(a), which shows that the mass gain of ZSM are higher than ZS. The plots of the square of the mass gain as a function of oxidation timer for ZSM and ZS are shown in Fig. 4(b), the linear relationship indicates that the oxidation follows parabolic behavior, suggesting that the oxidation is controlled by a diffusion process[19].

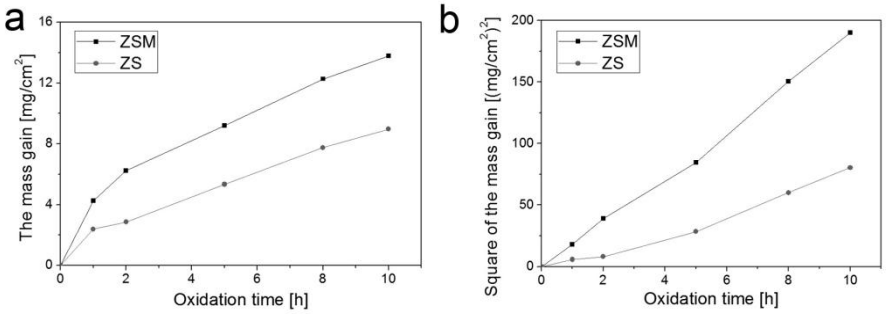

Fig. 4. The mass gain (a) and the square of the mass gain (b) change as a function of time for ZS and ZSM at 1500 ^{0}C in air.

After 10 h oxidation of ZSM and ZS at 1500 ^{0}C in air, a glossy and dense oxidation layer was both formed on the surface of ZSM and ZS. According to the placement during oxidation, the upper and lower surface of ZSM and ZS performed quite different that the oxidation layer on upper surface was smooth and transparent, but the oxidation layer on lower surface was rough with a lot of white phase. Therefore, the oxidation cross sections of the upper and lower surfaces of ZSM and ZS are analyzed separately.

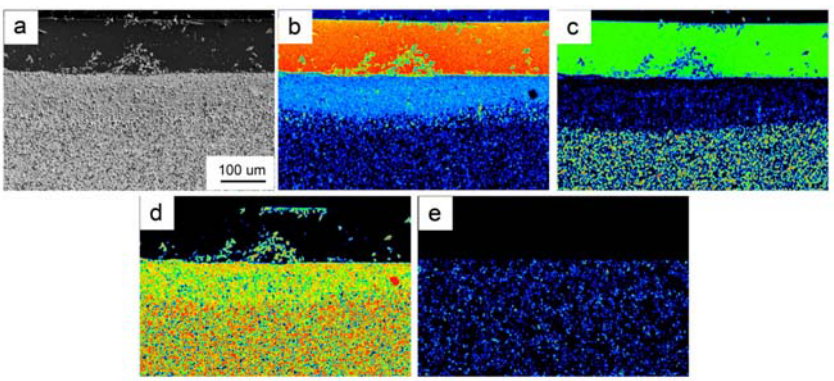

Fig. 5. The cross sectional image of the upper oxidation layer of the oxidized ZSM (a) and the elemental mapping of O, Si, Zr (b,c,d) at the same area, separately.

The cross sectional image of the upper oxidation layer of ZSM is shown in Fig. 5(a). According to the elemental mapping of O, Si, Zr, Mo at the same area (Fig. 5(b,c,d,e)), the oxidation layer could be divided into three layers and the oxidation depth (diffusion depth of O element into the ceramic) was 100-120 μm. The thickness of the first layer was about 120 μm, it was composed of SiO_2 and a small amount of ZrO_2, which was called "SiO_2 rich layer". The thickness of the second layer was about 70-90 μm, it was composed of ZrO_2 and a small amount of SiO_2, which was called "ZrO_2 rich layer". The thickness of the third layer was about 20~30 μm, it was composed of ZrB_2 and a small amount of ZrO_2, hardly containing Si, which was called "SiC depletion layer". The substrate close to the oxide layer was still composed of ZrB_2 and SiC, but the ZrB_2 phase had started to cleavage and was no longer a unbroken grain. Besides, Mo distributed evenly in the ZrO_2 rich layer, SiC depletion layer and substrate, there was no Mo distribution in SiO_2 rich layer.

The cross sectional image of the lower oxidation layer of ZSM and the elemental

mapping of O, Si, Zr, Mo at the same area (Fig. 6) showed that the oxidation layer could also be divided into three layers and the oxidation depth was 120~140 μm, thicker than the upper oxidation layer of ZSM. The main composition of each oxidation layer on lower surface was similar as the upper oxidation layer of ZSM. But the thickness of the first layer, called "SiO_2 rich layer", was 30~60 μm. The thickness of the second layer, called "ZrO_2 rich layer", was 100~110 μm. The thickness of the third layer, called "SiC depletion layer", was 20~30 μm. The ZrB_2 phase in the substrate close to the oxide layer had also started to cleavage, similar as the upper surface. Besides, Mo distributed also evenly in the ZrO_2 rich layer, SiC depletion layer and substrate, there was no Mo distribution in SiO_2 rich layer.

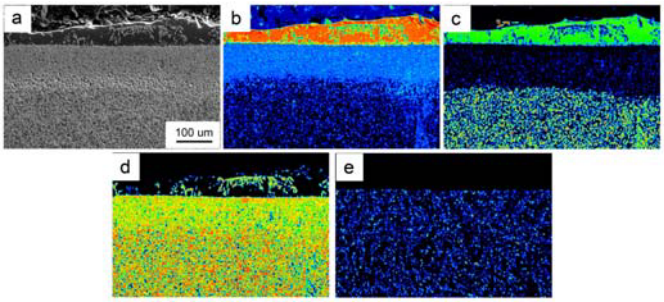

Fig. 6. The cross sectional image of the lower oxidation layer of the oxidized ZSM (a) and the elemental mapping of O, Si, Zr (b,c,d) at the same area, separately.

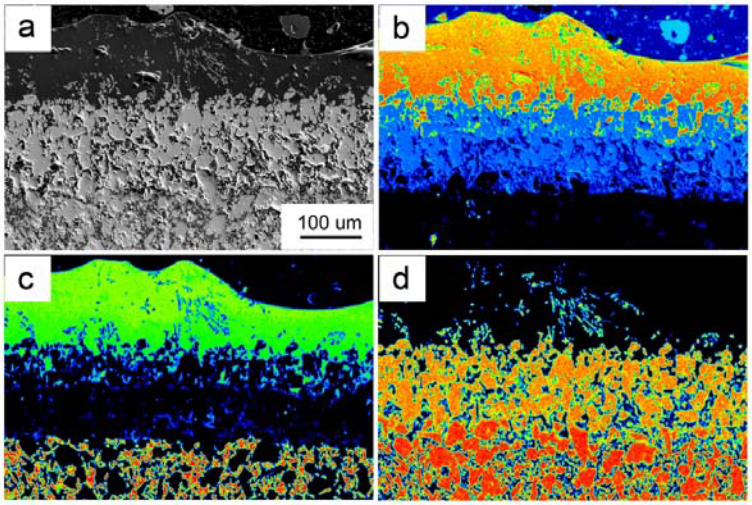

Fig. 7. The cross sectional image of the upper oxidation layer of the oxidized ZS (a) and the elemental mapping of O, Si, Zr (b,c,d) at the same area, separately.

The cross sectional image of the upper oxidation layer of ZS is shown in Fig. 7(a). According to the elemental mapping of O, Si, Zr (Fig. 7(b,c,d)), the oxidation layer could be divided into three layers and the oxidation depth was 150-160 μm. The thickness of the first layer was about 80~140 μm, it was composed of SiO_2 and a small amount of ZrO_2, which was called "SiO_2 rich layer". The thickness of the second layer was about 50~80 μm, it was composed of ZrO_2 and a small amount of SiO_2, which was called "ZrO_2 rich layer". The thickness of the third layer was about 80~100 μm, it was composed of ZrB_2 and a small

amount of ZrO_2, hardly containing Si, which was called "SiC depletion layer". The substrate close to the oxide layer was still composed of ZrB_2 and SiC, but the ZrB_2 phase had started to cleavage and was no longer a unbroken grain.

The cross sectional image of the lower oxidation layer of ZS and the elemental mapping of O, Si, Zr at the same area (Fig. 8) showed that the oxidation layer could also be divided into three layers and the oxidation depth was 250-300 μm, much thicker than the upper oxidation layer of ZS. The main composition of each oxidation layer on lower surface was similar as the upper oxidation layer. But the thickness of the first layer, called "SiO_2 rich layer", was 70~100 μm. The thickness of the second layer, called "ZrO_2 rich layer", was 200~230 μm. The thickness of the third layer, called "SiC depletion layer", was 80-100 μm. The ZrB_2 phase in substrate close to the oxide layer had also started to cleavage.

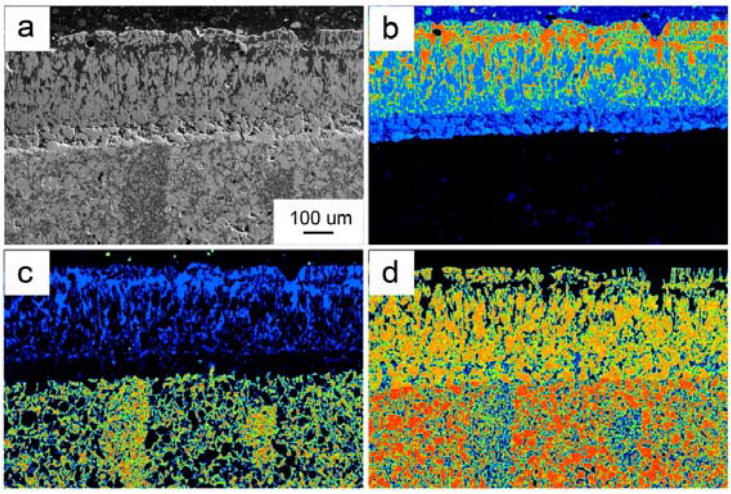

Fig. 8. The cross sectional image of the lower oxidation layer of the oxidized ZS (a) and the elemental mapping of O, Si, Zr (b,c,d) at the same area, separately.

Table 2 The Thicknesses Of Each Oxidation Layer On The Upper And Lower Surface Of The Oxidized Zsm And Zs

Material	SiO_2 rich layer [μm]	ZrO_2 rich layer [μm]	SiC depletion layer [μm]	Oxidation depth [μm]
ZSM upper surface	120	70-90	20-30	100-120
ZSM lower surface	30-60	100-110	20-30	120-140
ZS upper surface	80-140	50-80	80-100	150-160
ZS lower surface	70-100	200-230	80-100	250-300

According to the cross sectional images of ZSM and ZS (Fig. 5-8), the thicknesses of each oxidation layer on the upper and lower surface of ZSM and ZS were listed in Table 2, conclusions could be obtained as follows. The oxidation layers on upper and lower surface of ZSM and ZS were all composed of three layers: SiO_2 rich layer, ZrO_2 rich layer and SiC depletion layer. The substrate close to the oxide layer was still composed of ZrB_2 and SiC, but the ZrB_2 phase had started to cleavage and was no longer a unbroken grain. The compositions of the upper and lower oxidation layer of each sample were similar. But the oxidation depth of the upper surface was thinner than the lower surface in the same sample, the upper surface had thicker SiO_2 rich layer and thinner ZrO_2 rich layer than the lower surface, the thicknesses of SiC depletion layer on upper and lower surface were almost the same. This is due to the fluidity of SiO_2 at 1500 ^{0}C. On the upper surface, SiO_2 could stay on the surface to prevent the diffusion of O into the ceramic to oxidize; on the lower surface, fluid SiO_2 flowed down and left the surface, therefore O could diffuse deeper to oxidize. No matter the upper or lower surface, the oxidation depths of ZSM were all thinner than ZS. But after oxidation for 10 h at 1500 ^{0}C in air, the mass gain of ZSM (13.8 mg/cm^2) was much higher than ZS (9.0 mg/cm^2) which was because that SiO_2 oxidized on ZSM evaporated slower than ZS. In conclusion, the oxidation resistance of ZSM is better than ZS.

4. Summary

ZSM and ZS were successfully prepared via SPS sintering process at 1900 ^{0}C and characterized. MoB phase increasing the mechanical and chemical bonding force between different phases was formed in ZSM during SPS sintering. Therefore, the mechanical property of ZSM was improved significantly compared to ZS. The oxidation behavior of ZSM and ZS were carried out at 1500 ^{0}C in air. The oxide layers of ZSM and ZS were both composed of SiO_2 rich layer, ZrO_2 rich layer and SiC depletion layer. Due to the fluidity of SiO_2 at 1500 ^{0}C, the upper oxide layer in each sample was thinner than the lower oxide layer. Although the mass gain of ZSM was higher than ZS after 10 h oxidation, the oxidation depth of ZSM was thinner than ZS, which indicated that the oxidation resistance of ZSM was better than ZS. The results show that the mechanical property and the oxidation resistance of ZSM are both better than ZS, $MoSi_2$ is an effective additive to improve the mechanical property and oxidation resistance of ZrB_2-SiC ceramic.

References

1. S. R. Levine, E. J. Opila, M. C. Halbig, J. D. Kiser, M. Singh, J. A. Salem, Evaluation of ultra-high temperature ceramics for aeropropulsion use, J. Eur. Ceram. Soc. 22 (2002) 2757–2767.
2. J. Marschall, A. Chamberlain, D. Crunkleton, B. Rogers, Catalytic atom recombination on ZrB_2/SiC and HfB_2/SiC ultra-high temperature ceramic composites, J. Spacecraft Rockets. 41 (2004) 576–581.
3. C. Bartuli, T. Valente, M. Tului, Plasma spray deposition and high temperature characterization of ZrB_2-SiC protective coatings, Surf. Coat. Technol. 155 (2002) 260–273.
4. E. W. Neuman, G. E. Hilmas, W. G. Fahrenholtz, Mechanical behavior of zirconium diboride-silicon carbide ceramics at elevated temperature in air, J. Eur. Ceram. Soc. 33 (2013) 2889-2899.
5. L. Silvestroni, D. Sciti, Oxidation of ZrB_2 ceramics containing SiC as particles, whiskers, or short fibers, J. Am. Ceram. Soc. 94 (2011) 2796-2799.
6. [6] P. Hu, X. H. Zhang, J. C. Han, X. G. Luo, S. Y. Du, Effect of various additives on

the oxidation behavior of ZrB_2-based ultra-high-temperature Ceramics at 1800 degrees C, J. Am. Ceram. Soc. 93 (2010) 345–349.
7. F. Peng, R. F. Speyer, Oxidation resistance of fully dense ZrB_2 with SiC, TaB_2, and $TaSi_2$ Additives, J. Am. Ceram. Soc. 91 (2008) 1489–1494.
8. I. G. Talmy, J. A. Zaykoski, M. M. Opeka, High-temperature chemistry and oxidation of ZrB2 ceramics containing SiC, Si_3N_4, Ta_5Si_3, and $TaSi_2$, J. Am. Ceram. Soc. 91 (2008) 2250–2257.
9. Y. Wang, B. Ma, L. Li, L. An, Oxidation behavior of ZrB_2-SiC-TaC, J. Am. Ceram. Soc. 95 (2012) 374-378.
10. O. N. Grigoriev, B. A. Galanov, V. A. Lavrenko, A. D. Panasyuk, S. M. Ivanov, A. V. Koroteev, K. G. Nickel, Oxidation of ZrB_2-SiC-$ZrSi_2$[10] ceramics in oxygen, J. Eur. Ceram. Soc. 30 (2010) 2397-2405.
11. E. Opila, S. Levine, Oxidation of ZrB_2- and HfB_2-based ultra-high temperature ceramics: effect of Ta additions, J. Mater. Sci. 39 (2004) 5969-5977.
12. F. Monteverde, D. Alfano, R. Savino, Effects of LaB_6 addition on arc-jet convectively heated SiC-containing ZrB_2–based ultra-high temperature ceramics in high enthalpy supersonic airflows, Corros. Sci. 75 (2013) 443-453.
13. J. Lin, Mcrostructure and properties of 3Y-ZrO_2 fibers reinforced ultra high temperature ceramics, Harbin Institute of Technology, 2013.
14. W. Li, X. Zhang, C. Hong, W. Han, J. Han, Microstructure and mechanical properties of zirconia-toughened ZrB_2-$MoSi_2$ composites prepared by hot pressing, Scripta Mater. 60 (2009) 100-103.
15. C. W. Li, Y. M. Lin, M. F. Wang, C. A. Wang, Preparation and mechanical properties of ZrB_2–based ceramics using $MoSi_2$ as sintering aids, Front. Mater. Sci. China. 4 (2010) 271-275.
16. D. Sciti, F. Monteverde, S. Guicciardi, G Pezzotti, A. Bellosi, Microstructure and mechanical properties of ZrB_2-$MoSi_2$ ceramic composites produced by different sintering techniques, Mater. Sci. Eng. A. 434 (2006) 303-309.
17. D. Sciti, M. Brach, A. Bellosi, Oxidation behavior of a pressless sintered ZrB_2-$MoSi_2$ ceramic composite, J. Mater. Res. 20 (2005) 922-930.
18. D. Sciti, M. Brach, A. Bellosi, Long-term oxidation behavior and mechanical strength degradation of a pressurelessly sintered ZrB_2-$MoSi_2$ ceramic, Scripta Mater. 53 (2005) 1297-1302.
19. B. E. Deal, A. S. Grove, General relationship for the thermal oxidation of silicon, J. Appl. Phys. 36 (1965) 3770–3778.